THE OPERATING CHARACTERISTICS OF GEAR-TYPE COUPLINGS

by
Gerhardt Pahl
Professor and Engineer
Darmstadt Technical University
Darmstadt, West Germany

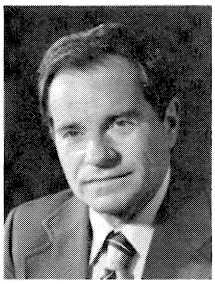

Gerhardt Pahl received his Ph.D. in Mechanical Engineering (Dr.-Ing.) at the Technical University of Darmstadt/Germany in 1955. The following decade he worked as a commissioning engineer for large steam-turbines and compressors and as a designer of those machines and their components for Brown Boveri Company. In 1965 Dr. Pahl became a full professor for machinery components and design principles at the university in Darmstadt. For several years he had been the dean of the Mechanical Engineering faculty of the Technical University of Darmstadt. His present research work concentrates on high-speed driving machines.

ABSTRACT

This paper describes in condensed form the results of a research project initiated by the Forschungskuratorium Maschinenbau e.V. and carried out at the Institut für Maschinenelemente und Konstruktionslehre of Darmstadt Technical University under the direction of Prof. Dr.-Ing. G. Pahl with the financial support of the Federal German Ministry of Economics via the Arbeitsgemeinschaft Industrieller Forschungsvereinigungen (AIF No. 2501). The research team for "gear-type couplings" headed by Ing. (grad) R. Wickl had overall responsibility for the project. The day-to-day work of the project was under the direction of Dipl.-Ing. R. Heinz and Dipl.-Ing. R. Fleiss. The contents and the calculation instructions are based on their theses.

INTRODUCTION

Gear-type couplings are commonly used as couplings between turbines and compressors at high speeds and in rolling mill plants at low speeds.

In the past, there has been a lack of any theoretical basis for estimating the friction which would allow to make a better assessment of wear and the axial thrust conditions.

KINEMATICS AND LOAD DISTRIBUTION OF THE GEAR-TYPE COUPLING

Figure 1 shows an experimental gear-type coupling as used on high-speed drives. Its particular features are a thin sleeve with straight-cut internal teeth and two hubs with slightly barrelled teeth or plain teeth with rounded ends.

If there is any angular or parallel misalignment between the shafts to be joined, one coupling hub is inclined at an angle δ_{HS} to the sleeve as shown in Figure 2.

At position 1 the hub tooth is in a *tilted position*, 90° later at position 2, it is in a *pivoted position*. During rotation each hub tooth passes twice through a pure tilted position and twice

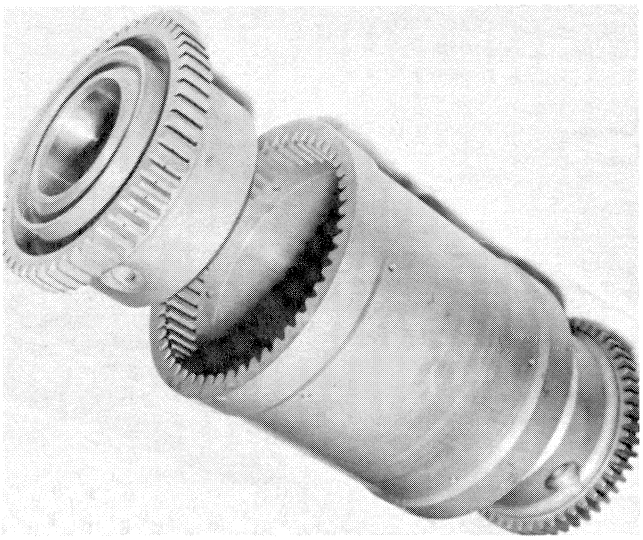

Figure 1. Gear-Type Coupling With Circulated Oil Lubrication.

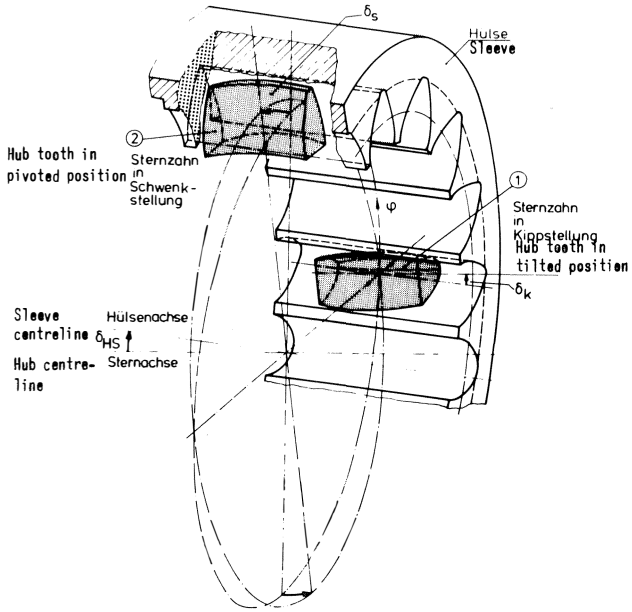

Figure 2. Typical Tooth Positions.

through a pure pivoted position per revolution. In between, the positions are a mixture of tilt and pivot motions.

When the coupling is deflected by an angle δ_{HS}, displacement occurs between the hub and sleeve teeth tangentially to

the pitch circle. This tangential displacement f_t is at its greatest in the tilt zones. This is where the teeth first bear when the torque transmission begins. As a result, the load distribution is not constant over the circumference when the coupling is deflected as seen in Figure 3. The greater the deflection, the greater the concentration of load in the tilt zones.

The pitch errors which are approximately of the same order of magnitude as the tangential displacement itself, are superimposed on the tangential displacement. This means further non-uniform loading of the teeth over the circumference. Figure 4 shows this condition.

If a separate centering element does not determine the sleeve position, the sleeve will adjust its position in relation to the hub freely according to the forces acting upon it. This process is generally associated with eccentric displacement of the sleeve mass, which causes inertia forces as a function of the speed.

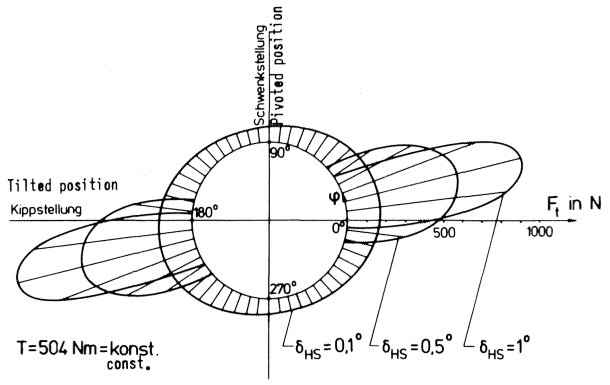

Figure 3. Load Distribution With Different Angles of Deflection δ_{HS}.

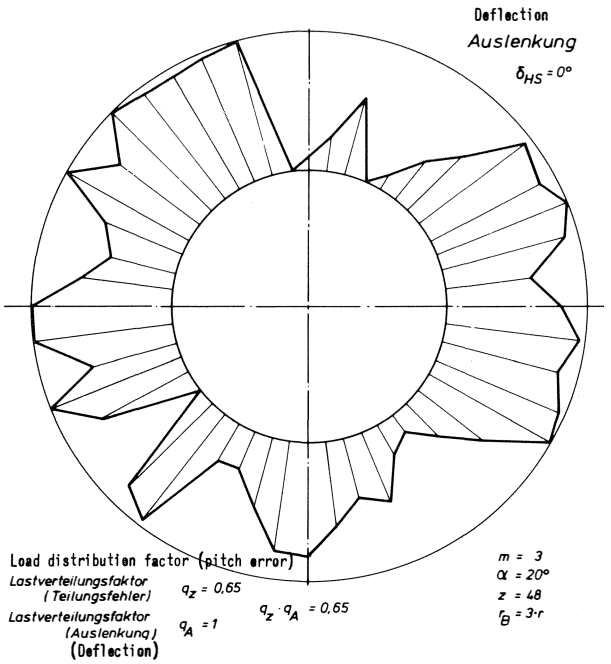

Figure 4. Load Distribution With Pitch Errors, No Coupling Deflection.

The magnitude and direction of this displacement are derived from load distribution theory which describes the tooth forces of the coupling according to the loading, kinematics (deflection and speed) and pitch error distribution.

The displacement of the sleeve and the resulting forces can be calculated as a function of the coupling and operating parameters by an iterative method using a computer program [2, 3]. Figure 5 shows the vertical inertia forces of the sleeve calculated for different deflection angles and speeds over one revolution. It can be seen that the forces at $16\delta_{HS} = 0.1°$ deflection are still sineform whereas with increasing deflection there is three times the excitation caused by the pitch error distribution.

Figure 6 shows, for the width of the tooth, the sliding velocity v_G — governing the temperature rise and wear of the tooth flanks — and the hydrodynamically effective velocity v_H — governing the formation of the lubricating film. Also shown is the tangential displacement f_t which is the governing factor for the tooth force with no pitch errors or inertia forces.

The sliding velocity v_G is at a maximum at the points of reversal of tooth contact, whereas the hydrodynamically-effective velocity v_H is at minimum. The tangential displacement f_t, and therefore the tooth force, is greatest at the points of reversal. Knowledge of these conditions is an essential first step towards assessing the formation of the lubricating film and the friction conditions.

CONTACT SURFACE OVERLAP

The supply of lubricant, however, is highly dependent on the contact surface overlap

$$Pu = \frac{a_{HZ}}{s_{1\,max}}$$

and is typical of many oscillating rolling contact conditions.

The contact surface overlap is the ratio of half the Hertzian contact surface width a_{HZ} to the maximum travel $s_{1\,max}$ of the point of contact on the flank of the hub tooth as seen in Figure 7.

The following three cases are important:

Case 1: Pu < 1 The travel of the point of contact $s_{1\,max}$ is greater than half the Hertzian contact

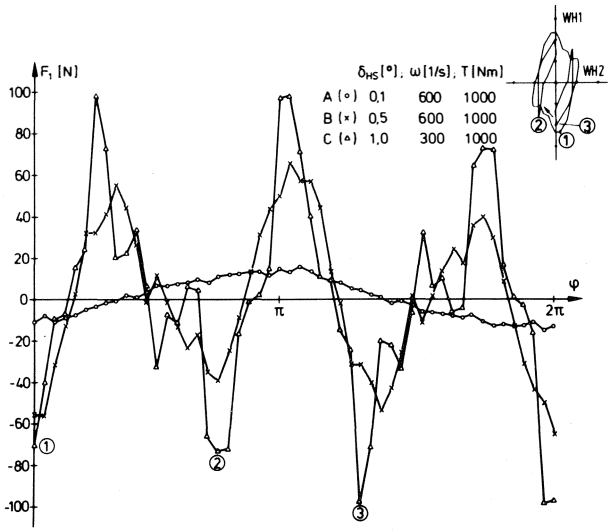

Figure 5. Calculated Vertical Inertia Forces of the Sleeve.

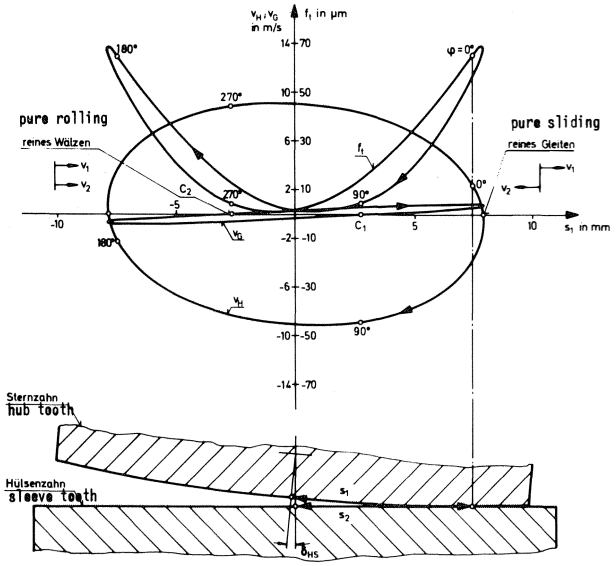

Figure 6. Kinematic Conditions at the Circular Arc Tooth.

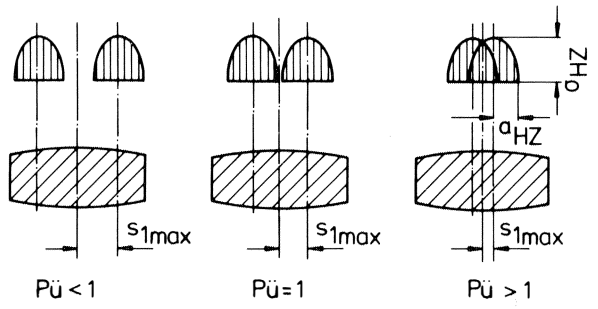

Figure 7. Contact Surface Overlap for Various Operating Conditions.

surface width a_{HZ}. The lubricant has access to all parts of the tooth flank.

Case 2: Pu = 1 Limit case $s_{1\,max} = a_{HZ\,max}$. Lubricant access is still possible but difficult.

Case 3: Pu > 1 The travel of the point of contact $s_{1\,max}$ is less than half the Hertzian contact surface width. Part of the flank is continuously overlapped. Lubricant access to the flank is difficult to inadequate.

LOAD CAPACITY COEFFICIENT

In regard to the formation of the lubricating film, it has been experimentally determined that due to the delayed build-up and collapse of the lubricating film, especially with the couplings having a large curvature radius of the tooth flank, the maximum thickness is only attained shortly before the points of reversal.

A steady-state approximation calculation with a shortened inlet gap was carried out and the hydrodynamic load capacity F_{HD} possible for a given lubricating film thickness of 1 um calculated.

The hydrodynamic load capacity F_{HD} is thus seen in Figure 8.

$$F_{HD} = \frac{2.447 \times h \times \eta \times v_H \times R_e}{\text{trag}\ h_o} \times f(b_{1x})$$

$|\leftarrow$ Reynolds solution $\rightarrow|\leftarrow$ Effect of shortened gap length b_{1x}

h_{bear} = *load carrying tooth length*

η = *viscosity*

v_H = *hydrodynamic effective velocity* (δ_{HS}, ω, ϵ)

R_e = *pressure line radius*

h_o = *lubricating film thickness*

$f(b_{1x})$ = *function of the length of the inlet gap, which reduces the load capacity by 50% or more depending on pressure line radius*

Fig. 8. Hydrodynamic Load Capacity.

Hence the load capacity coefficient Tr is determined:
Load capacity coefficient

$$Tr = \frac{\text{hydrodynamic load capacity } F_{HD}}{\text{specified max. normal tooth force } F_{n\,max}}$$

Due to the assumptions and simplifications contained in the calculation, the load capacity must be quoted as a coefficient which indicates what hydrodynamic pressure can be expected.

FRICTION CONDITIONS AND FRICTION COEFFICIENT RANGES

By combining the contact surface overlap Pu (coefficient for lubricant supply) and the load capacity coefficient Tr (coefficient for lubricating film formation) in one diagram as seen in Figure 9, it is possible to determine the friction conditions in a gear-type coupling.

The contact surface overlap Pu is drawn horizontally. The greater the contact surface overlap, the worse the supply of lubricant.

The load capacity coefficient Tr is drawn vertically to an ascending scale. The greater the value of Tr, the better the lubricating film.

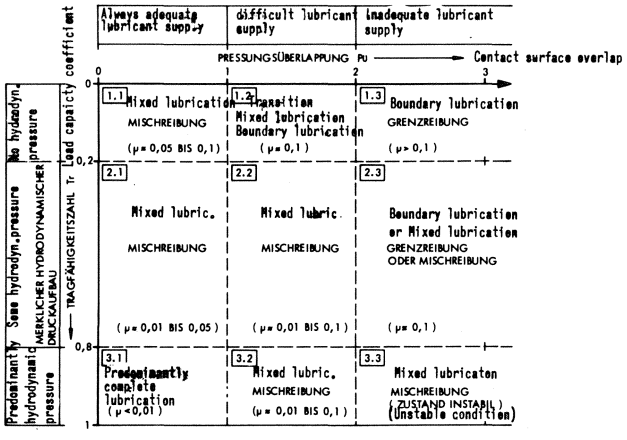

Figure 9. Friction Conditions in Gear-Type Couplings.

The results, confirmed by tests, are areas of different friction conditions and different friction coefficient ranges where the boundaries are fluid.

e.g. area 1.1

A contact surface overlap Pu< 1 always means an adequate supply of lubricant. A load capacity coefficient Tr < 0.2 means that there is no detectable hydrodynamic pressure. The teeth run in the mixed lubrication area. The coefficient of friction is between 0.05 and 0.1. With increasing contact surface overlap Pu, the supply of lubricant becomes more and more difficult and at Pu > 2, the area of boundary lubrication with $\mu > 0.1$ has been entered.

If the load capacity coefficient Tr increases at constant contact surface overlap Pu, there is a transition from area 1.1 to area 3.1 with predominantly complete lubrication with $\mu <$ 0.01.

In the mixed lubrication area (area 1.1 of Figure 7), the coefficient of friction μ is clearly dependent on the sliding velocity v_G.

Figure 10 shows μ as a function of the maximum sliding velocity $v_{G\,max}$ and therefore as a result of the deflection angle times speed. The causes are probably micro-hydrodynamic effects.

The important relationship between the coefficient of friction μ and the deflection angle δ_{HS} — and therefore also once again the effect of contact pressure overlap Pu and load capacity coefficient Tr — is shown in Figure 11.

Two curves are shown: curve 1 refers to a heavily crowned tooth and curve 2 to a slightly crowned tooth.

Curve 1 shows a minimum at approximately $\delta_{HS} = 0.4°$ with a friction coefficient of $\mu = 0.05$. The mating teeth run in the area of mixed lubrication. With diminishing deflection, the coefficient of friction increases because the sliding velocity decreases and the contact surface overlap increases until it reaches the area of boundary lubrication with μ exceeding 0.1.

With large deflection, the same coupling runs in the area of less contact surface overlap. With diminishing deflection, more teeth carry the load, the load capacity Tr rises slightly but remains relatively small because the tooth is heavily crowned and remains in the mixed lubrication area. The smaller the deflection, the greater the contact surface overlap and therefore the coefficient of friction and the coupling enters the boundary lubrication area.

Curve 2 has a minimum at $\delta_{HS} = 0.1°$ with $\mu<0.01$. Due to the large flank curvature radius, the lubrication condition of the tooth is predominantly in the area of complete lubrication. With a smaller angle of deflection, the coefficient of friction rises sharply and quickly enters the area of boundary lubrication $\mu \geqslant 0.01$.

At its greatest deflection, the coupling runs in the area of low contact surface overlap with a high load capacity (almost complete lubrication). If the deflection is reduced, the load capacity falls sharply after approximately $\delta_{HS} = 0.1°$ and the contact surface overlap increases. The coupling quickly enters the area of *mixed lubrication and boundary lubrication* with a correspondingly high coefficient of friction.

Hence, the friction condition diagram allows estimation of the friction condition and coefficient of friction range and to determine the optimum operating range.

AXIAL THRUST

The design of gear-type couplings also allows shaft misalignment in the axial direction. However, in the past, the magnitude of the resulting resistance to sliding has been unclear. The axial thrust of the coupling must be taken by the respective thrust bearings. There were a variety of preconceptions of the axial forces involved leading to the adoption of different coefficients of friction for the tooth normal force between 0 and 0.3.

Description of the Mechanism

Two operating conditions can give rise to axial thrust in a gear-type coupling carrying a torsional load: the axial displacement of the teeth in contact with each other (e.g. caused by thermal expansion of a shaft) and parallel misalignment of two coupled shafts (the so-called Z condition). Both conditions can also occur at the same time.

A general expression for the axial thrust F_{ax} as a function of the tooth normal forces F_n^i, the coefficient μ and the relative velocity v_r between the tooth flanks is as follows:

$$F_{ax} = \sum F_n^i \cdot \frac{\vec{v}_r}{/v_r/} \mu$$

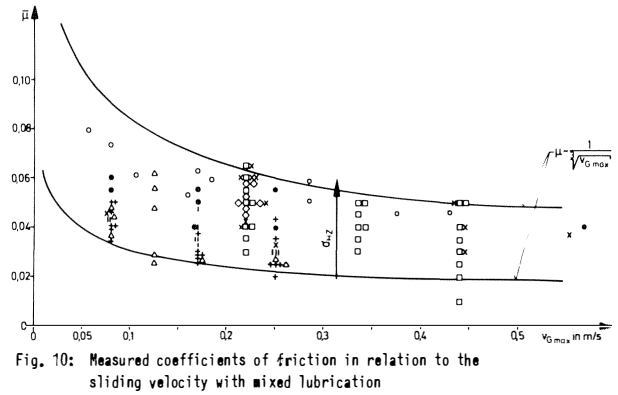

Fig. 10: Measured coefficients of friction in relation to the sliding velocity with mixed lubrication

Figure 10. Measured Coefficients of Friction in Relation to the Sliding Velocity With Mixed Lubrication.

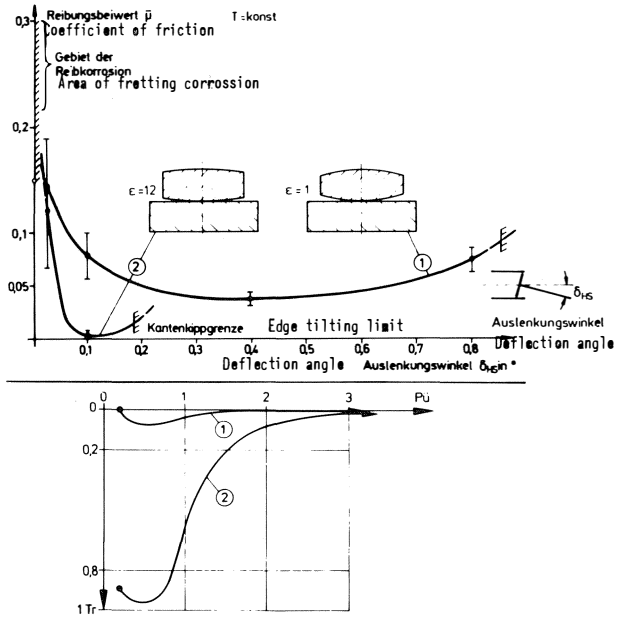

Figure 11. Variation of Friction Coefficient and Friction Conditions.

Axial Displacement

With coaxial shafts this condition is a trivial matter. The same axial sliding velocity v_{ax}, causing a friction force F_R in the same direction, prevails at each pair of teeth. F_R is the sum of all tooth normal forces F_n^i and is proportional to the coefficient of friction.

The axial force can then be stated thus:

$$F_{ax} \frac{T}{r_o \cos \alpha} \mu$$

T = Torque

r_o – Pitch circle radius

α = Pressure angle

Parallel Misalignment

If there is parallel misalignment between the shafts, the result is a sliding velocity between the pairs of teeth in the tilting zones of the coupling teeth which is determined by the deflection angle between the hub and sleeve centrelines and the speed. At the pitch circle, the hub and sleeve have the same magnitude of circumferential velocity $v = r\omega$ but it differs in direction at sleeve and hub.

This results in a relative velocity between the pairs of teeth which is called the sliding velocity v_G as shown in Figure 12.

During one revolution, the hub and sleeve teeth displace themselves twice but in different directions to each other.

The friction forces caused by v_G act in the same direction. If the gear-type coupling is simplified to one pair of load-bearing teeth in the tilt zones in each case, the force conditions can be represented as in Figure 13 (tooth normal forces not shown). The tooth normal force causes a friction force F_R in the same axial direction as v_G, i.e. it reverses its direction around the circumference. As a result, there is an unbalanced moment about the 2 axis $M_2 = 2F_R d_o$ acting on the sleeve.

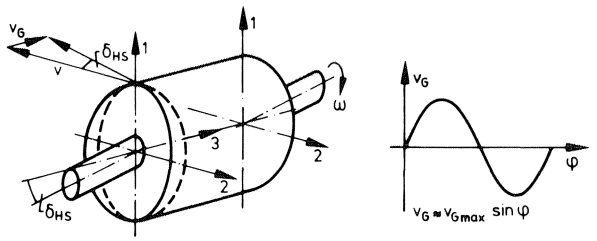

Figure 12. Sliding Velocity v_G of the Coupling Teeth.

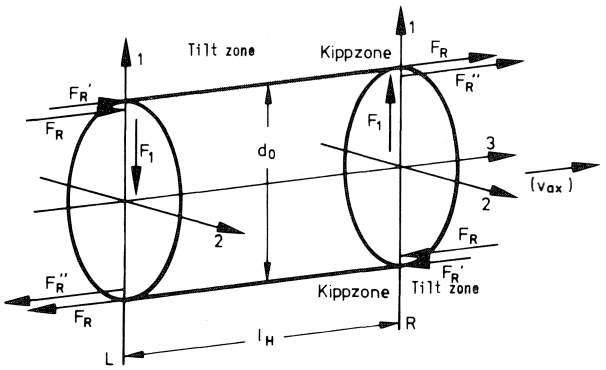

Figure 13. Axial Force Mechanism With Shafts in Parallel Misalignment.

This moment is counteracted by a force

$$F_1 = M_2/I_H = 2F_R \frac{d_o}{I_H}$$

However, F_1 can only be applied by changing the tooth normal forces. (For the coupling, this means that the sleeve rotates by a small amount about an axis in 2 dimensional).

In plane L, the upper tooth normal force decreases, the lower increases; whereas in plane R the reverse takes place. Different tooth normal forces also cause different friction forces. In the left-hand plane L turns into F_R, the now smaller force $F_{R'}$, whereas below the larger friction force $F_{R''}$ is produced. In the right-hand half, the situation is reversed.

From the force balance in the 3 dimensional (axial), it can be seen that although the axial forces on the sleeve are balanced, those on the shaft end are not; the force difference $F_{ax} = F_{R'} - F_{R''}$ must be borne by the thrust bearings of the shafts.

From this simplified mechanical model, it can also be seen that the ratio d_o/I_H affects the axial thrust conditions in the *parallel misalignment situation.*

The other shaft arrangement which must be considered is when both shafts are at an angle to each other (the so-called M arrangement). In this case, the friction forces revolve in one of the two planes and for reasons of symmetry, the sleeve is in equilibrium without the tooth normal forces being changed, i.e. there are no axial forces acting on the shaft ends.

Theoretical Results

Explanation of the
Axial Force Distribution

At deflection $\delta_{HS} = 0$, the axial force is solely determined by the effective tooth normal forces and the prevailing coefficient of friction μ which, depending on the relative velocity between the pairs of teeth, changes from the static friction value to the sliding friction value and causes a relatively high axial thrust. With very small deflections δ_{HS} and simultaneous axial motion with a velocity $v_{ax} > v_G$ as seen in Figure 14a, all friction forces remain unidirectional. The axial thrust is then determined as before from the tooth normal forces and friction coefficient μ alone and retain its value.

As the deflection δ_{HS} increases, the sliding velocity v_G will exceed at some of the pairs of teeth, the directionally opposite axial velocity v_{ax}, which causes the effective friction forces to reverse in direction as seen in Figure 14b. The friction force acting on the shaft end is thereby reduced considerably. With even greater deflection, v_G is so high that the axial velocity v_{ax} can be neglected as seen in Figure 14c. The friction forces at the pairs of teeth cease almost completely and the axial thrust on the shaft approaches zero.

Calculated Axial Thrust

In the following Figures 15 and 16, axial thrust values calculated by means of a computer program have been plotted against the deflection angle δ_{HS} for the coupling under study having the principal data z = 52, m = 3 mm, d_o = 156 mm, $\epsilon = r_b/r_o = 1$.

ϵ = Crowning ratio

r_b = Pitch line crowning radius

r_o = Pitch circle radius

The following applies to all figures:

Curve 1:	$v_{ax} = 0$ mm/s	Family of curves
2:	= 0.5 mm/s	A : T = 1000 Nm
3:	= 1 mm/s	B : T = 3000 Nm
4:	= 2 mm/s	C : T = 5000 Nm

The remaining parameters are as follows:

μ = constant for all curves of a diagram

	μ	ω(1/s)
Fig. 15	0.2	50
Fig. 16	0.2	200

It can be seen that the axial forces are a function of torque and that at higher speeds the axial thrust over δ_{HS} falls rapidly because the ratio v_G/v_{ax} increases as in Figure 14. Another very important factor can also be ascertained from Figures 15 and 16; even at ω = 200 rev/s ($\approx$ 2000 rev/min) with 0.05° deflection, the axial thrust which can be transmitted has fallen to less than 10% of the maximum value despite constant coefficients of friction.

The variation in axial thrust produced by the Z arrangement (see Figure 13) in relation to the coefficient of friction μ is shown in Figure 17. The torsional moment and deflection angle are constant.

Experimental Results

The conditions described have been checked by experiment; Figure 18. The sharp drop predicted when the deflection angle δ_{HS} is greater than 0.05° is clearly demonstrated. For the true coaxial position, the high axial thrust values rose as predicted by the previous conventional method of calculation.

A gear-type coupling should, for medium values of deflection, be operated so that in accordance with the results obtained by Heinz [1], it runs in an area of low axial thrust with

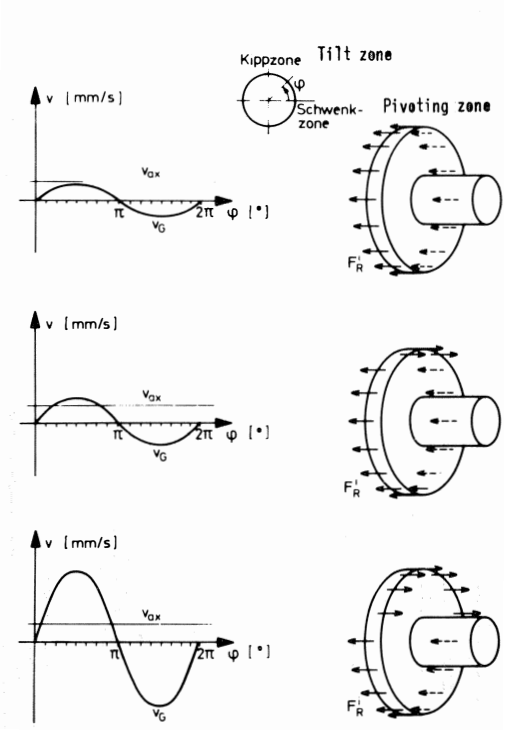

Figure 14. Axial Thrust as a Function of Sliding Velocity v_G and Axial Velocity v_{ax}.

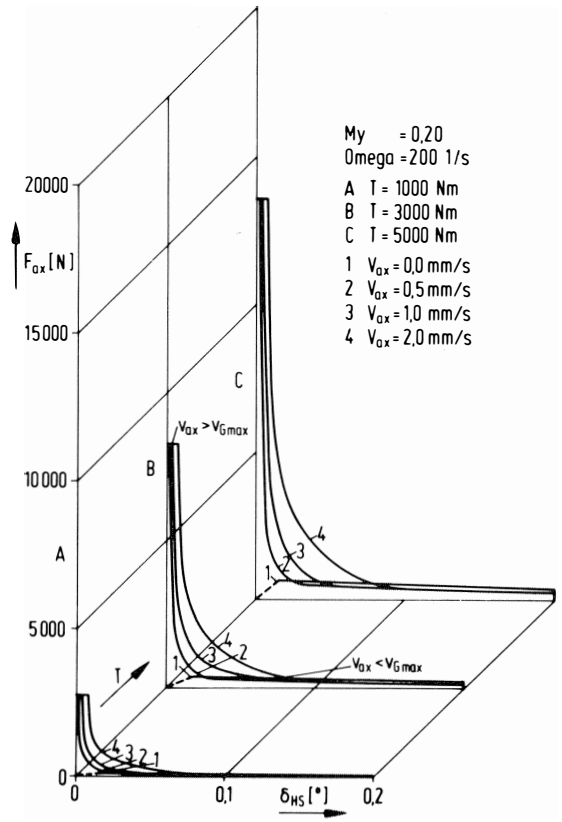

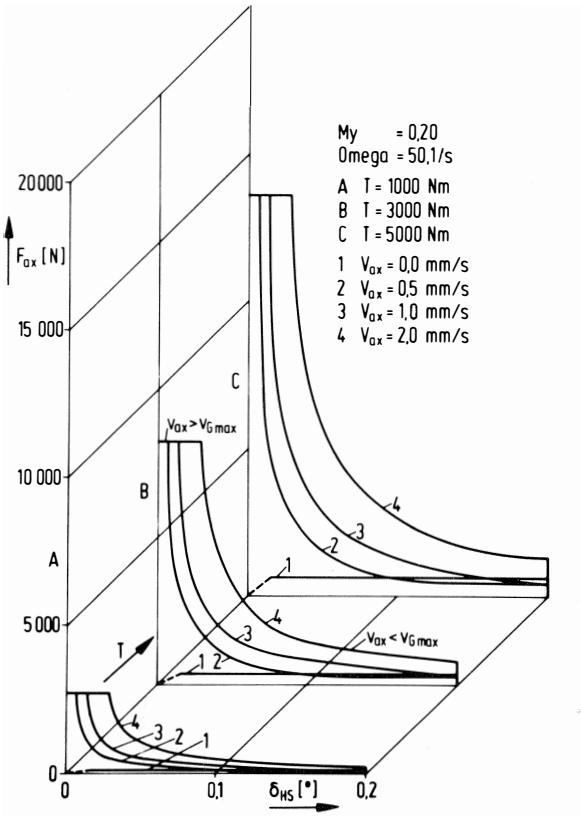

Figures 15 and 16. Calculated Axial Thrust of a Gear-Type Coupling.

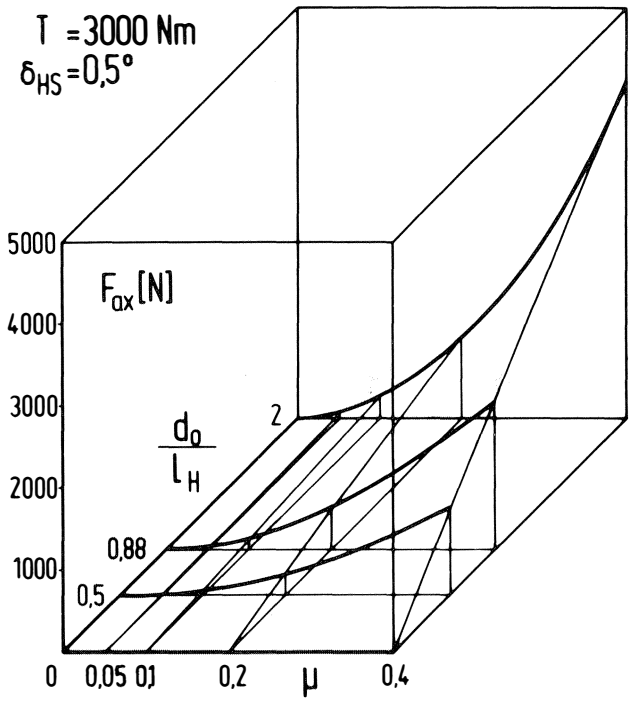

Figure 17. Self-Induced Axial Thrust of a Gear-Type Coupling With Parallel Misaligned Shafts.

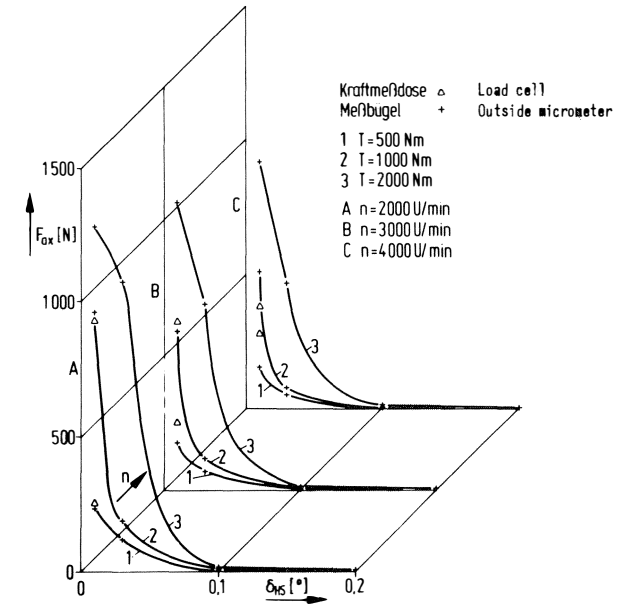

Figure 18. Measured Axial Thrust of a Gear-Type Coupling.

simultaneously favorable lubricating film formation of low friction values and low wear. Calculation instructions derived from this study have been prepared for practical use.

In conclusion, the following recommendations can be given for the design and operating of gear-type couplings:

The crowning ratio ϵ (pitch line crowning radius r_b/pitch circle radius r_o) and the deflection angle δ_{HS} should be so matched that the contact surface overlap Pu is always less than unity. The load capacity coefficient Tr should then be as high as possible. The results will then generally be found to be in the region of minimum friction according to Figure 11, as well as obtaining a small but sufficiently large deflection of the coupling which leads to the expectation of very small axial forces according to Figures 15 and 16.

REFERENCES

1. Heinz, Rudolf, Untersuchung der Kraft- und Reibungsverhaltnisse in Zahnkupplungen fur grosse Leistungen. Thesis, Darmstadt Technical University 1977.
2. Fleiss, Rainer, Radial- und Axialverhalten von Zahnkupplungen. Thesis, Darmstadt Technical University 1977.
3. Fleiss R. und G. Pahl, Radial- und Axialkrafte beim Betrieb von Zahnkupplungen. VDI-Report No. 299, Dusseldorf, BDI-Verlag 1977.